

## Transport Properties of Sodium close to the Melting Point

G. Fritsch and E. Lüscher

*Physik-Department, Technische Universität München, München, Germany*

(Received 29 March 1971)

Close to the melting point the thermal conductivity and the electrical resistivity of sodium (99.99 at. % with 100 and 200 ppm potassium) were measured simultaneously in the same sample. A steep rise was found in the thermal conductivity whereas the electrical resistivity showed no departure from the expected behavior. Also no difference could be detected between the polycrystalline and single-crystalline samples. The results are discussed in terms of the impurity content, of a pure-first-order transition, and of an instability point of the solid state. Some arguments are given to support the instability hypotheses.

### I. INTRODUCTION

The nature of first-order thermodynamic phase transitions has recently attracted much interest. Among the properties which have been measured are the specific heats of the alkali metals sodium,<sup>1</sup> rubidium, and cesium,<sup>2</sup> of body-centered-cubic (bcc) helium,<sup>3</sup> and of high-purity gallium,<sup>4</sup> the diffusion coefficients of indium,<sup>5</sup> tin,<sup>6</sup> and sodium,<sup>7</sup> ultrasonic attenuation in tin,<sup>8</sup> and the specific volume of sodium.<sup>9</sup> The conclusion may be drawn from all those data that there is some intrinsic or impurity-dependent effect close to the melting transition.

To examine this point further it was decided to measure the transport properties very close to the melting point. High-purity sodium (99.99 at. %) was chosen as a test substance, because the crystal structure is bcc and therefore easy to handle theoretically. The electronic structure is also well known.<sup>10</sup> Thus studies of a pure lattice transition seem to be possible, the Fermi surface being a sphere in both the solid and liquid states. Electrical and thermal conductivities are reported in this paper. The measurements were done using single- and polycrystalline-sodium samples with different impurity contents. Three samples were doped with 100 ppm (mole) potassium and one 200 ppm. The other impurities detected were Mg < 20 ppm, Fe < 5 ppm, and Ca < 5 ppm, as stated by the supplier.<sup>11</sup> The oxygen content should be smaller than 5 ppm.<sup>12</sup>

The present paper is organized as follows. Section II contains a brief survey of the main approaches to a theory of melting. Effects due to impurities are considered in Sec. III. The apparatus and method of measurement are explained shortly in Sec. IV, whereas Sec. V presents the main results of this paper. In Sec. VI, several possible mechanisms for the anomalous thermal conductivity are suggested including some arguments which support an instability-point hypothesis.

### II. SURVEY OF APPROACHES TO MELTING THEORY

It has been proven by Lee and Yang<sup>13</sup> that statis-

tical mechanics is capable of dealing with the problem of different phases in a many-particle system. These authors were able to show that in the thermodynamic limit of an infinite system the Gibbs free energy is a continuous function of pressure and temperature and that a first-order phase transition is determined by discontinuities in the first partial derivatives with respect to the stated variables. However for a real interacting system it is almost impossible to calculate the exact Gibbs free energy for the whole range of the variables from first principles. Thus this function is evaluated separately for the different phases by introducing suitable approximations. The two-phase equilibrium curve  $\hat{p} = \hat{p}(T)$  can be derived in this case by equating two of these Gibbs free energies. In finite systems, the metastable states of superheating and supercooling are allowed. To what extent these states can be reached is governed by rate theories of seed growing.<sup>14</sup> Pre- and after-melting phenomena are also possible, according to the Frenkel-Bartenev<sup>15</sup> theory. These authors introduced the argument into the theory that a certain amount of the metastable phase, specified by a parameter  $\mu$ , is already present in the stable region (heterophase fluctuations).

In the Lee and Yang theory, the magnitudes of the second partial derivatives of the Gibbs free energy  $G$  at a point, where a first-order transition occurs, remain undetermined. It is normally accepted that these derivatives are finite and do not show any extraordinary behavior. However one can not exclude the possibility that for the compressibility  $\kappa_T$ :

$$\kappa_T = - \left( \frac{\partial^2 G}{\partial p^2} \right)_T / V \quad (1)$$

and/or for the specific heat at constant pressure  $c_p$ :

$$c_p = T \left( \frac{\partial^2 G}{\partial T^2} \right)_p \quad (2)$$

or, generally speaking, that any one of the partial

second derivatives of the thermodynamic potentials,<sup>16</sup>  $G$  being a special case of these potentials, are diverging if the transition point is approached from below, i. e., from the solid side of the melting transition. This special assumption is called the instability hypothesis of the solid phase. It is based on the physical argument that the melting transition is primarily caused by an instability of the solid phase. Possible mechanisms for such an instability are discussed later on in Sec. VI.

To the authors knowledge, no theories for the solid-liquid transition do exist, relating the relative position of the instability limit of a phase—determined by divergences of the second partial derivatives of the general thermodynamic potentials—to that of the metastability limit, fixed by the discontinuity of the first partial derivatives of the Gibbs free energy. At the present stage of the theory, a possible coincidence or a closeness of both limits, a necessary condition for the instability hypothesis (see Fig. 1), can only be deduced from experimental results. Some of these, concerning the alkaline metals, are collected in Table I. It may be stated that other bcc metals than the alkaline ones also fit closely into the same pattern.<sup>17</sup> Typical solid-state parameters, such as the activation energy for diffusion  $Q_a$ , the expansion coefficient  $\alpha$ , and the formation enthalpy of vacancies  $H_f^v$ , are directly related to the melting temperature. But the most striking evidence in this context is the Lindemann<sup>17</sup> melting rule, which holds for the five alkali metals as well as for a lot of other metals. Table I gives the Lindemann constant  $c$  which should be the same for all substances with the same lattice structure.<sup>18</sup>

According to the stated instability hypothesis, one can propose the following picture of the melting

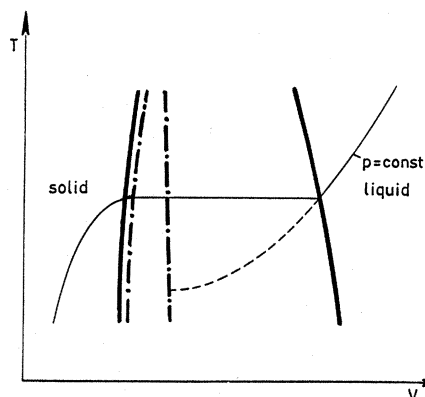


FIG. 1. The  $T$ - $V$  diagram proposed for the melting transition. Heavy lines indicate the metastability limits, whereas the dashed-dotted lines give the stability limits of the solid and liquid phases, respectively. Thin lines correspond to the equilibrium isobar. For further comments see text.

transition. The instability limit of the solid phase in the temperature-volume diagram of Fig. 1 lies very close to (or coincides in the most extreme case with) the metastability limit, whereas the instability limit of the liquid phase is separated distinctly from the corresponding metastability limit (see also note added in proof). Thus it is evident that this transition looks like a higher-order one from the solid side, with no super-heating, while on the liquid side the normal behavior of a first-order transition is exhibited. Large supercooling is therefore possible. The failure of the usual Maxwell equal-area construction is clearly seen in this case. But that objection is not serious, as there is no sound foundation for this procedure.

TABLE I. Correlation between solid-state properties and the melting point of the alkali metals.  $T_m$ : melting point;  $Q_a$ : activation energy for self-diffusion;  $\alpha$ : volume expansion coefficient;  $H_f^v$ : single-vacancy formation energy; and  $c$ : Lindemann constant.

Metal	$T_m$ (K) <sup>b</sup>	$Q_a$ (eV) <sup>c,d</sup>	$\alpha$ $10^{-4}$ (K <sup>-1</sup> )	$H_f^v$ (eV) <sup>d</sup>	$c^a$	$Q_a/T_m$ $10^{-3}$ (eV/K)	$\alpha T_m$ $10^{-2}$	$H_f^v/T_m$ $10^3$ (eV/K)
Li	453.7	0.562	1.7 <sup>e</sup>	0.40	3.2	1.24	7.7	0.88
Na	371.0	0.450	2.2 <sup>f</sup>	0.42	3.8	1.21	8.2	1.13
K	336.4	0.425	2.5 <sup>f</sup>	0.39	3.3	1.265	8.4	1.16
Rb	312.6	0.411	2.7 <sup>f</sup>		3.9	1.313	8.4	
Cs	302.9		2.9 <sup>e,f</sup>		3.6		8.8	

<sup>a</sup>J. J. Gilvarry, Phys. Rev. **102**, 308 (1956).

<sup>b</sup>Handbook of Chemistry and Physics, 48th ed. (The Chemical Rubber Co., Cleveland, Ohio, 1967). Absolute temperature and temperature differences are indicated by the symbol "K" (Kelvin), where  $10^{-3}$  K = 1 mK. Sometimes temperature is also given in °C.

<sup>c</sup>J. N. Mundy (unpublished).

<sup>d</sup>R. C. Brown, J. Worster, N. H. March, R. C. Perrin, and R. Bullough, AERE HL Report No. 70/2825 (1970) (unpublished).

<sup>e</sup>G. Borelius, in *Solid State Physics*, edited by F. Seitz and D. Turnbull (Academic, New York, 1958), Vol. 6.

<sup>f</sup>B. Eckstein, Phys. Status Solidi **20**, 83 (1967).

## III. IMPURITIES

In discussing pre-melting phenomena the impurity question has to be an important one. A lot of the reported data (see Table I of Ref. 6) are strongly dependent on the impurity content of the samples. As far as impurity effects are understood<sup>1,2</sup> we can separate the impurities into two groups distinguished by their relative solubilities in the host metal: (i) Soluble impurities are responsible for mainly two effects. Normally the melting point is lowered and broadened to a melting region, depending on the distribution factor  $k$ .<sup>1</sup> This factor is defined as the ratio of the saturation concentration of the impurity in the solid phase to that in the liquid phase at the melting temperature. It can be deduced from the slopes of the solidus and liquidus lines in the two substances' phase diagram for small impurity contents.

The following equation can be derived from thermodynamic arguments<sup>1</sup> for small impurity concentrations:

$$T_{m\gamma} = T_{mp} - RT_{mp}^2 x L_m^{-1} [\gamma + k/(1-k)]^{-1}, \quad (3)$$

where  $T_{mp}$  is the melting point of the pure substance;  $R$ , the gas constant;  $L_m$ , the latent heat of melting;  $x$ , the impurity concentration in the solid (mole per mole);  $\gamma$ , the ratio of the molten part of the sample to the total sample mass; and  $k$ , the distribution factor as defined above. The solidus line is given by  $\gamma$  equal to zero; whereas  $\gamma$  equal to one corresponds to the liquidus line. The width of the melting region is calculated from Eq. (3) to be

$$T_{m1} - T_{m0} = RT_{mp}^2 x(1-k)^2/(L_mk), \quad (4)$$

and the melting point depression is

$$T_{mp} - T_{m1} = RT_{mp}^2 x(1-k)/L_m. \quad (5)$$

Additional effects on the defect properties at high temperatures are also generated by impurities.<sup>9</sup>

(ii) Nonsoluble impurities are clustered at inner (grain boundaries) and outer surfaces of the crystal but only if there is full equilibrium. Each cluster is then surrounded by a small layer of liquid, in which those impurities are dissolved to some extent. This effect can be deduced from Eqs. (3) and (4) by setting  $k$  equal to zero. It is seen that at every temperature below the melting point a certain part of the sample is molten. The situation is not altered if there is a homogeneous impurity distribution resulting from a rapidly solidified melt. In this nonequilibrium case, the melting transition is also smeared out. After a short time the solid contains pockets of the liquid phase at regions where the impurities had assembled by diffusion. Thus large premelting effects are easy to detect if nonsoluble impurities are present.

## IV. APPARATUS AND METHOD OF MEASUREMENT

The measurements were made in a thermostat, described elsewhere.<sup>19</sup> The sodium sample was contained in a stainless-steel tube with the following dimensions: length 120 mm, wall thickness 0.1 mm, and diameter 6 mm. Thermal conductivities were measured by a quasistatic method with very small temperature gradients (<30 mK). Variations in the heat capacity of the sample are included in the data-analysis procedure. Corrections were also made for parallel heat conduction and for radiation. Very low heating rates (less than 50 mK per 24 h) were used for changing the absolute temperature. A measurement at a given temperature was checked with additional runs at the same temperature, allowing for various cooling times (6–24 h) between two runs. In the limits of the stated errors no systematic variations of the results could be detected. Further experimental details may be found in a previous paper.<sup>20</sup> The electrical conductivity was measured simultaneously in the same sample using a Kelvin-bridge arrangement integrated into the thermostat to minimize thermopower distortion.

Statistical errors are estimated to be 3% for the electrical conductivity and about 6% for the thermal conductivity measurements in the "normal" region, outside the steep rise. Depending on the smallness of the temperature gradient in the "fast rise" region, the errors there grow up to about 20% (see Fig. 6).

## V. RESULTS

Results for the thermal and electrical conductivities are plotted in Figs. 2–5. The temperature region covered extends from 0.5 K below, up to 0.15 K above the starting point of melting ( $T_{m0}$ ). These data points are corrected for averaging due to the temperature predifference  $\delta T_{pre}$  and due to the measurement interval. The predifference  $\delta T_{pre}$  is defined to be the temperature difference across the sample, before the heat flux for the measurement  $q_0$  was switched on. This difference was adjusted in such a manner that it equals about half the temperature rise due to the heat flux  $q_0$ . That procedure gives optimal conditions for the data reduction. The numbers for the predifferences are also listed in the figures. They indicate that no changes occur when these values are altered. Data points shown are derived from two single crystals (samples 2 and 3) and from polycrystals (samples 1 and 4). Orientations and impurity contents are also stated in the figures. A glance at the electrical resistivity reveals that the impurity effect of melting-zone broadening is clearly visible. Identifying the first kink in these curves with the starting point of melting  $T_{m0}$  and the second one with the

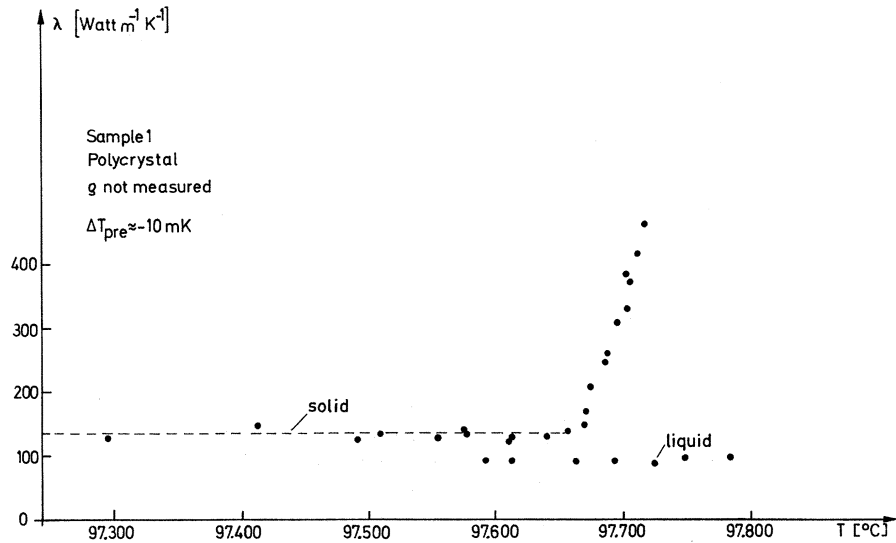


FIG. 2. Thermal conductivity of the polycrystalline sample 1 with an impurity content of 100 ppm (mole) potassium. Temperature scale from direct quartz thermometer readings, not corrected.

end point  $T_{m1}$ , one can calculate the impurity content and the melting-point depression with the aid of Eqs. (4) and (5). The absolute temperatures given in the Figs. 3–5 are derived from these calculations and the assumption that the melting point of the pure substance is 97.830 °C.<sup>1</sup> The resulting temperature scale is in good agreement with the absolute-temperature determination by a high-resolution quartz thermometer.<sup>21</sup> The calculated impurity con-

tents are also within the limit of the stated contaminations in the samples 1–3. Sample 4 shows a scattering of data points in the region where the steep rise calculated from the known impurity content should occur. Further comments on the point are made in Table II and in the discussion.

Supercooling in both electrical and thermal conductivities is also shown in these figures. It was possible to maintain these metastable states as long

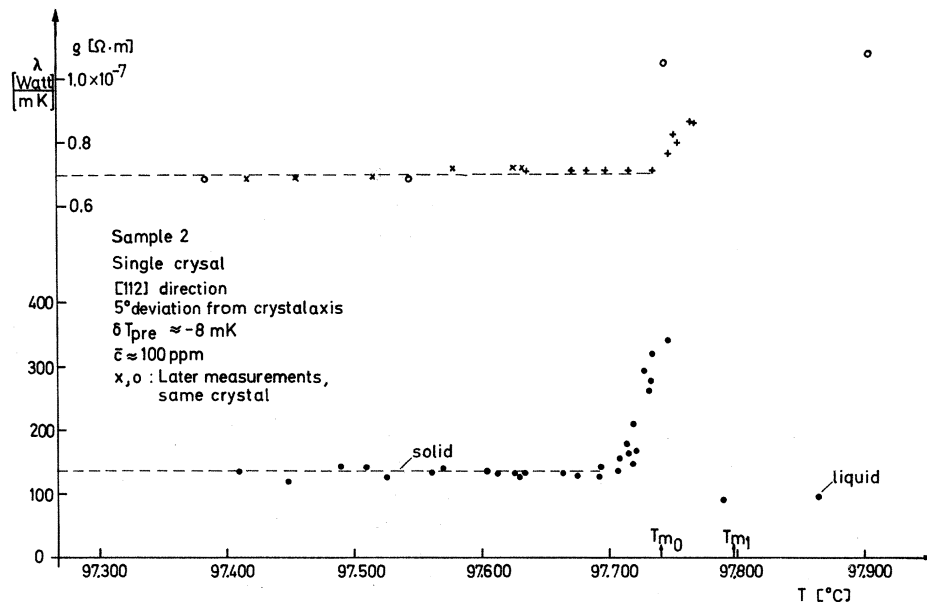


FIG. 3. Thermal conductivity and electrical resistivity of the single crystalline sample 2. Temperature scale corrected through the width of the melting region. Melting point of pure sodium is accepted to be 97.830 °C. Stated impurity content 100 ppm (mole).

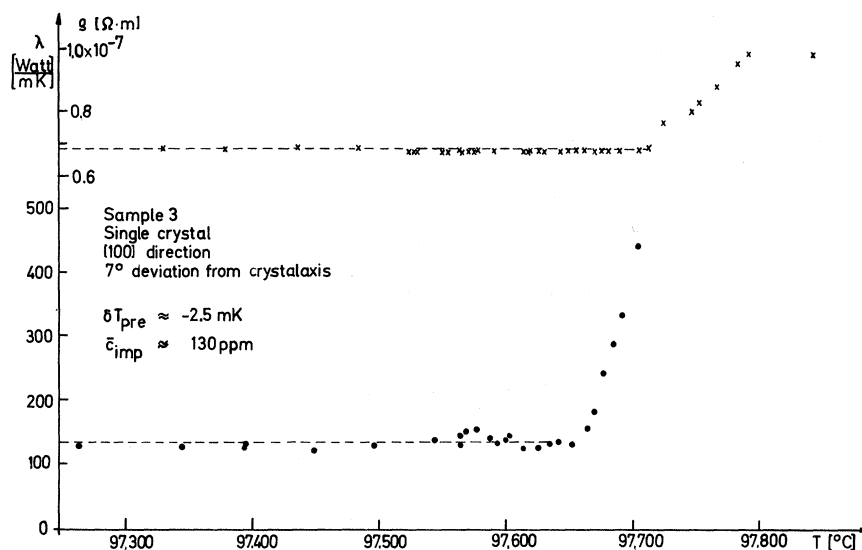


FIG. 4. Thermal conductivity and electrical resistivity of the single crystalline sample 3. For comments see Fig. 3.

as three days. In contrast, superheating was never seen. The dashed lines shown are extrapolations of fitted straight lines from the measurements from 32 °C up to the melting point.<sup>20</sup>

#### VI. DISCUSSION

First we would like to discuss the steep rise of the thermal conductivity prior to melting in view of the impurity content of the samples. Nonsoluble impurities are not detected and likely not present. This point of view is supported by two arguments.

The impurity contents calculated from the width of the melting region are in good agreement with the stated impurity contents as are the evaluated melting point depressions with the temperature scale. That point was already discussed in Sec. V. Second, the partial melting of the sample would have been seen in a rise of the electrical resistivity which was not observed (except in sample 4, however; see discussion below).

The major impurity, potassium, is soluble at these concentrations in the solid and liquid phase. (See

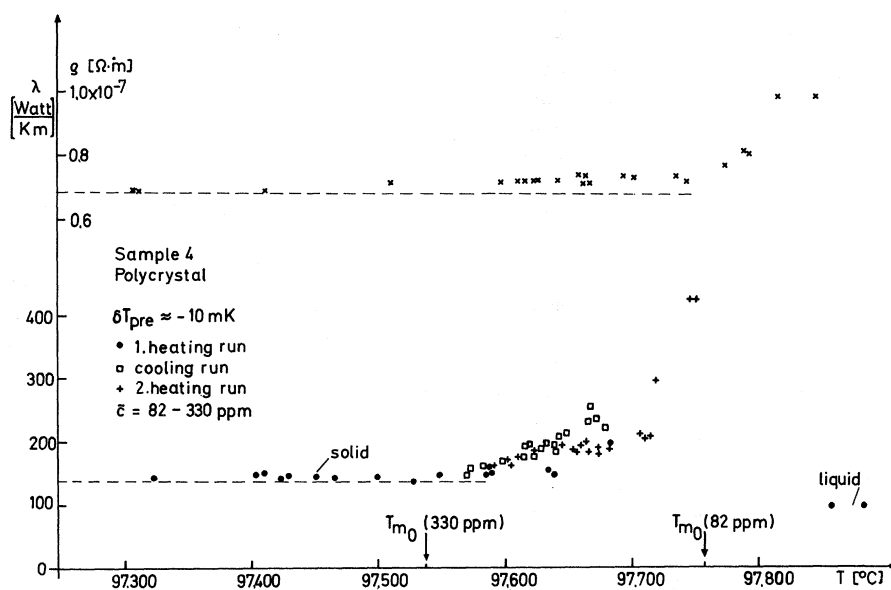


FIG. 5. Thermal conductivity and electrical resistivity of the polycrystalline sample 4. Stated impurity content 200 ppm (mole) potassium. For further comments see Fig. 3 and text.

TABLE II. Calculated impurity contents and starting points of melting, using  $k=0.33$  (Ref. 22) and  $T_{m0}=97.830^\circ\text{C}$  [from Eqs. (4) and (5)].

Sample No.	Width of the melting region (mK)	Impurity content [ppm (mole)]	Starting point of melting ( $^\circ\text{C}$ )
1	Not measured		
2	$58 \pm 5$	100	97.75
3	$77 \pm 6$	130	97.71
4	$48 \pm 6$	60	97.76
4	...	330	97.54

sodium-potassium-phase diagram.<sup>22</sup>) No contaminations were introduced during handling as is shown by the agreement between the stated and measured impurity contents (Table II). Spatial inhomogeneous impurity distributions can cause different starting points of melting  $T_{m0}$  in different parts of the sample. This effect can easily arise during solidification due to zone refinement effects. To avoid such a distribution one has to wait for equilibrium in the liquid state, which has a much higher diffusion coefficient than the solid. The solidification must occur with such a crystallization velocity that the diffusion is now ineffective in establishing equilibrium during this process. An almost homogeneous impurity distribution will result.<sup>14</sup>

Looking at the present experiments, an inhomogeneous distribution can be ruled out by two arguments. First, if there exists a locally lower melting point, it must be seen in a rise of the electrical resistivity. The ratio of the resistivities of the liquid to the solid state is about 1.5. A molten percentage as low as about 6% can be detected by this method (see discussion of sample 4). Second, any small variation of the heat capacity of the sample will not influence the thermal conductivity measurements, this effect being incorporated in the data analysis.<sup>20</sup> Using the diffusion coefficient<sup>7</sup> of solid sodium, one can show that small inhomogeneities of some millimeters in magnitude will disappear typically with a time constant of about 10 h. This time is short compared with the over-all time of measurement of about three months.

Now let us discuss the anomalous behaviour of sample 4. Inspection of Fig. 5 shows a time-dependent behavior of the thermal conductivity, which can be taken as an indication of strong diffusion effects. The reason for such a behavior is possibly an inhomogeneous impurity distribution. The electrical resistivity shows also a small rise in this region. One can explain the experimental results assuming a higher impurity concentration of about 330 ppm potassium at one end of the sample and a lower one in the middle and the other end. The first smaller rise is due to premelting effects in

the first zone, while the final steep rise belongs to the lower impurity content. The two starting points of melting are indicated by arrows in Fig. 5.

At this point in the discussion one should emphasize that the observed high thermal conductivities prior to melting could be caused by unknown impurity effects or could be explained by an intrinsic property of the pure material. This point cannot be clarified however by the present experiments. Additional work at purer sodium and especially on high-purity metals is necessary to get further information. Other low-melting metals such as indium and gallium are available at high purity but there are also a lot of additional difficulties connected with the interpretation of the data, because these metals possess complex lattice structures and also complex electronic systems. The following discussion is therefore based on both possibilities and gives some arguments for the impurity, as well as for the pure-material hypothesis.

At first one could be tempted to interpret the experimental results in terms of the Frenkel-Bartenev theory, mentioned in Sec. II. The mass parameter, which characterizes the fraction of the metastable phase inside the stable one, can be determined from volume expansion measurements.<sup>9</sup> But this theory can never account for the rise in the thermal conductivity because the liquid value is smaller by a factor of about 0.65 in comparison to the solid one at  $97^\circ\text{C}$ . A second possibility is to think in terms of a soft-mode behavior, analogous to that which was proposed by Alder *et al.*<sup>3</sup> to explain their results on the specific heat of bcc solid helium. Despite the fact that helium is an extreme quantum substance, the mechanisms introduced by these authors seem also possible for nonquantum materials. Such a soft mode could either be identified with a special transverse phonon<sup>23</sup> at wave vector  $\vec{q} \gtrsim 0$ , i.e., a sound wave, or with a longitudinal or transversal phonon at wave vector  $\vec{q}$  close to a reciprocal lattice vector,<sup>24</sup> at least in principle. These latter vibrational modes are termed "umklapp" phonons. The list of candidates must be viewed in the light of the physical background, that these excitations are absent or are largely modified in the liquid.<sup>25</sup> Possible mechanisms for such a softening could be the introduction of a large concentration of vacancies as well as of an appreciable amount of impurity atoms into the well-ordered lattice array. In the present experiments, the concentration of vacancies at the melting point<sup>9</sup> is about  $10^{-3}$ , whereas the impurity concentration is about  $10^{-4}$ . This can be taken as an indication that, roughly speaking, the impurity effect may be in the same order of magnitude as the vacancy one. Also the coupling of the phonons to one another via the anharmonic interaction could play an important role in the breakdown of the long-range order.

At first glance, however, the soft-mode hypothesis seems not to be adequate to explain the anomalous behavior of the thermal conductivity, as phonons with small- $\vec{q}$  vectors are pure sound waves which do not contribute very much to the transport of heat. But this difficulty can be removed by the following argument: Separation of the thermal conductivity into a lattice part  $\lambda_l$  and an electronic part  $\lambda_e$ , with the aid of the Wiedemann-Franz law, shows that only the lattice part diverges.<sup>26</sup> Now the lattice part can be looked upon to be a sum of a phonon part  $\lambda_{ph}$  and of a diffusion part  $\lambda_d$ . Let us now concentrate on the diffusion part. Nonequilibrium thermodynamics provides a link between diffusion and thermal conductivity through the coupling of heat and particle flow, caused by gradients in the temperature and in the chemical potential, respectively. To get a feeling for the magnitude of  $\lambda_d$  we assume to a first approximation a vacancy-type diffusion<sup>27</sup>

$$\lambda_d = -Dc(Q_t + H_f^v)H_f^v / (k_B T^2 f), \quad (6)$$

where  $D$  is the diffusion coefficient,  $Q_t$  the heat of transport,  $H_f^v$  the enthalpy of formation of a single vacancy,  $c$  the concentration of vacancies, and  $f$  the correlation factor. Taking into account the results of some experiments<sup>5</sup> which report a steep rise in the diffusion coefficient prior to melting, we assume  $D$  to be as large as in the liquid. Further,  $c \approx 10^{-3}$ ,<sup>9</sup>  $Q_t \approx -0.1$  eV,<sup>28</sup>  $H_f^v \approx 0.4$  eV.<sup>9</sup> The result for  $f \approx 1$  is

$$\lambda_d \approx -10^{-3} [J/(msK)]. \quad (7)$$

Thus  $\lambda_d$  has the wrong sign, as long as the modulus of  $Q_t$  is less than  $H_f^v$ .  $\lambda_d$  is also negligible in comparison to the phonon part  $\lambda_{ph}$ . A vacancy-type diffusion is therefore not adequate to explain the reported results.

Now returning to the soft-mode behavior, it should be pointed out that a largely enhanced diffusion could be caused by the softening effect. The lower the energy, the larger is the individual occupation number of the special phonon and the larger are the amplitudes of the corresponding vibration. Therefore the soft phonons destroy the regular lattice array (the long-range order), as the particles participating in this excitation are no longer confined to their lattice sites. Thus large units consisting of many particles are allowed to diffuse through the remaining "crystal." Nothing is known on the effectiveness of such a mechanism for the thermal transport. Accepting this argument it is proposed that the steep rise in the thermal conductivity is produced by a largely enhanced diffusion part  $\lambda_d$  of the lattice thermal conductivity. That conclusion is supported by results, obtained theoretically by Kadanoff *et al.*<sup>29</sup> at the liquid-gas critical point  $T_c$ . They calculated the temperature dependence of transport properties close to  $T_c$ . Regarding the heat transport by sound waves, these authors find a divergence according to  $\ln(T - T_c)$ , whereas for the heat transport by viscous-flow modes they

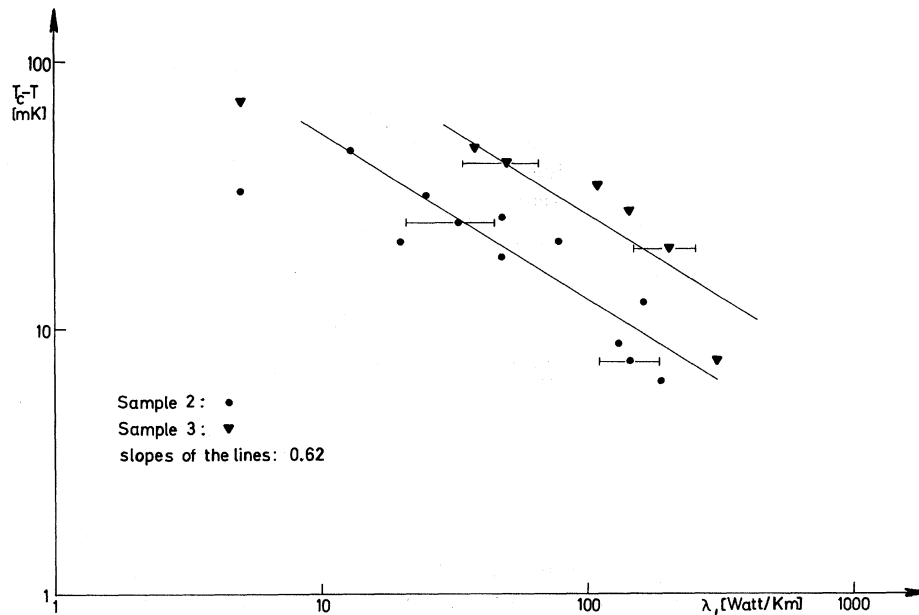


FIG. 6. Examination of the power-law behavior of the lattice part of the thermal conductivity close to the melting point. Hand-fitted lines with a slope of 0.62 are also shown for comparison with the theory. For further comments see text.

obtained a divergence characterized by  $|T - T_c|^{-2/3}$ . If one assumes a behavior of the thermal conductivity at the instability limit which resembles that at the liquid-gas critical point, one can now compare the data with the theoretical prediction. This is done, identifying  $T_c$  with the starting point of melting  $T_{m0}$  as defined in Sec. III. Figure 6 shows that the data points are scattered around a line with a slope of roughly  $-\frac{2}{3}$ . However, in view of the errors involved, the agreement may be fortuitous, but it can be stated that a logarithmic divergence is not adequate to fit the data.

To check the consistency of the proposed mechanism, let us examine its influence on the electrical conductivity. Using the Ziman formula,<sup>30</sup> one can make plausible that for monovalent metals, such as sodium, the electrical conductivity  $\sigma$  is neither influenced by long-wavelength homophase fluctuations nor by the softening of the "umklapp" phonons to first order. This equation was proposed for the liquid state but it can also be applied to a solid using averaged quantities:

$$\sigma^{-1} \sim \int_0^{2k_F} |V(q)|^2 S(q) q^3 dq, \quad (8)$$

where  $V(q)$  is the electron-ion pseudopotential,  $S(q)$  is the averaged static structure function,  $k_F$  the Fermi wave vector, and  $q$  the phonon wave vector. In the limit  $q \rightarrow 0$ ,  $S(q)$  becomes proportional to the compressibility. Inspection of Eq. (8) shows that only if the compressibility diverges there might be some effect, largely damped down by the factor  $q^3$  and by the integration. As the Fermi surface of sodium is well inside the first Brillouin zone and as the integration extends only to  $2k_F$ , no effect from a possible "umklapp"-phonon softening is to be expected. These phonons are centered around reciprocal lattice vectors, which are well outside the range of integration. The assumption that prior to melting a lattice instability may occur—as discussed above from the point of view of the transport properties—is also supported from

volume expansion measurements at sodium.<sup>9</sup> These data can be interpreted to give a power-law behavior for the expansion coefficient at constant pressure. The exponent was determined to be  $-0.34 \pm 0.14$ . Thus the expansion coefficient diverges if the melting point is approached from the solid side, whereas at the liquid side of the transition no anomaly occurs.

All these observations can be explained in a natural way, assuming that the instability limit of the solid phase is close to the metastability limit, as was already discussed in Sec. II. On the other hand there exists no high-temperature theory of the true stability limit of the solid phase,<sup>31</sup> thus no comparison between the experimental results presented in this paper and theoretical calculations can be made.

## VII. SUMMARY AND CONCLUSION

It is shown that prior to melting there is a rise in the lattice part of the thermal conductivity. Several possible mechanisms were proposed and discussed, favoring a connection between melting and an instability point of the solid phase. Further studies of static and dynamic properties of simple systems are necessary in the immediate vicinity of the melting point, to lend support to or to reject this proposal.

*Note added in proof.* Recently T. Schneider *et al.*<sup>32</sup> were able to show by theoretical considerations and by computer experiments that a soft-mode behaviour exists in a supercooled liquid, which could be identified with the stability limit of the liquid state.

## ACKNOWLEDGMENTS

The authors are indebted to many colleagues for stimulating discussions. The help of Dr. Goldman, who read the manuscript and gave valuable comments, is gratefully acknowledged.

<sup>1</sup>D. L. Martin, Phys. Rev. **154**, 571 (1967).

<sup>2</sup>D. L. Martin, Can. J. Phys. **48**, 1327 (1970).

<sup>3</sup>B. J. Alder, W. R. Gardner, J. K. Hoffer, N. E. Phillips, and D. A. Young, Phys. Rev. Letters **21**, 732 (1968).

<sup>4</sup>J. Jach and F. Sebba, Trans. Faraday Soc. **50**, 226 (1954); O. A. Boedtker, R. C. La Force, W. B. Kendall, and S. F. Ravit, *ibid.* **61**, 665 (1965).

<sup>5</sup>R. E. Eckert and H. G. Drickamer, J. Chem. Phys. **20**, 13 (1952).

<sup>6</sup>R. H. Packwood and P. J. Black, Proc. Phys. Soc. (London) **86**, 653 (1965); A. J. F. Boyle, D. St. P. Punbury, C. E. Edwards, and H. E. Hall, *ibid.* **77**, 129 (1960).

<sup>7</sup>J. N. Mundy, L. W. Barr, and F. A. Smith, Phil. Mag. **14**, 785 (1966).

<sup>8</sup>K. G. Plass, Acustica **1**, 240 (1963).

<sup>9</sup>M. Ritter, G. Fritsch, and E. Lüscher, J. Appl. Phys. **41**, 5071 (1970).

<sup>10</sup>M. J. G. Lee, Proc. Roy. Soc. (London) **A295**, 440 (1966).

<sup>11</sup>N. V. Hollandse-Billiton (unpublished).

<sup>12</sup>H. Beisswenger and S. Dorner, J. Nucl. Mater. **28**, 297 (1968).

<sup>13</sup>T. D. Lee and C. N. Yang, Phys. Rev. **87**, 404 (1952); **87**, 410 (1952).

<sup>14</sup>C. Knight, *The Freezing of Supercooled Liquids* (Van Nostrand, Princeton, N.J., 1967).

<sup>15</sup>J. Frenkel, *Kinetic Theory of Liquids* (Clarendon, Oxford, England, 1947).

<sup>16</sup>G. Falk, *Theoretische Physik, II Thermodynamik, Heidelberger Taschenbücher* (Springer Verlag, Berlin, 1968).

<sup>17</sup>R. A. Ubbelohde, *Melting and Crystal Structure*



(Clarendon, Oxford, England, 1965).

<sup>18</sup>V. V. Goldman, *J. Phys. Chem. Solids* **30**, 1019 (1968).

<sup>19</sup>G. Fritsch, *Z. Angew. Math. Phys.* **22**, 505 (1967).

<sup>20</sup>G. Fritsch and E. Lüscher, *J. Phys. Chem. Solids* (to be published).

<sup>21</sup>Fa. Hewlett-Packard, Palo Alto, Calif.

<sup>22</sup>D. K. C. Mac Donald, W. B. Pearson, and L. T. Towle, *Can. J. Phys.* **34**, 389 (1956).

<sup>23</sup>This point of view is only possible if one can define a suitable extension of the low-temperature phonon into the high-temperature region. Neutron scattering experiments give phonon peaks right up to the melting point, a result which supports the possibility of such an extension.

<sup>24</sup>G. Meissner, *Phys. Rev. B* **1**, 1822 (1970).

<sup>25</sup>S. C. Jain, N. S. Saxena, and R. C. Bhandari, *J. Chem. Phys.* **52**, 4629 (1970); K. S. Singwi, K. Sköld, and M. P. Tosi, *Phys. Rev. A* **1**, 454 (1970).

<sup>26</sup>The assumption of the validity of the Wiedemann-Franz

law is not implausible as the electrical conductivity shows no anomalous effects prior to melting.

<sup>27</sup>R. A. Oriani, *J. Phys. Chem. Solids* **30**, 339 (1969).

<sup>28</sup>G. A. Sullivan, *Phys. Rev.* **154**, 605 (1967).

<sup>29</sup>L. P. Kadanoff and J. Swift, *Phys. Rev.* **166**, 89 (1968).

<sup>30</sup>M. P. Greene and W. Kohn, *Phys. Rev.* **137**, A513 (1965).

<sup>31</sup>Compare however the results of a computer experiment by W. G. Hoover, and F. H. Ree [*J. Chem. Phys.* **49**, 3609 (1968)] on hard spheres. They find an instability point in their solid phase results, characterized by a diverging compressibility. The instability is above the thermodynamic transition temperature (metastability limit), but this shift could be produced by the nature of the approximations used.

<sup>32</sup>T. Schneider, R. Brout, H. Thomas, and Z. Feder (unpublished).

## Noninteracting Fermi Gas in a Square-Well Potential\*

Carl E. Nash†

*The Department of Physics, The University of North Carolina,  
Chapel Hill, North Carolina 27514*

(Received 26 April 1971)

The problem of a noninteracting Fermi gas in a finite square-well potential is solved analytically in the limit that the well becomes infinitely wide. The errors of previous authors using this model as a first approximation to the problem of a simple metal with surfaces are pointed out.

A very simple model which has been used to represent electrons in a simple metal with surfaces is a noninteracting Fermi gas in a square-well potential. Bardeen<sup>1</sup> was probably the first to use this model in his paper on the theory of the work function. He used the wave functions of this model to calculate the exchange potential across the surface. Huntington<sup>2</sup> used the same model to calculate the surface energy of a simple metal in a first approximation. More recently, Lang and Kohn<sup>3</sup> based their more sophisticated calculation of the surface energy and the work function of some metals at least in part on this model, and on the work of Bardeen and of Huntington. It is the purpose of this paper to calculate the exact analytic solution to this problem, since, as will be shown, incorrect assumptions about the density of states and the normalization of the wave functions of the problem have led to errors in some of the above work.

We shall define the problem somewhat differently than has been done previously in order to show the exact quantum-mechanical solution of the Schrödinger equation with the proper boundary conditions. The coordinates of the problem are such that the  $x$  axis is perpendicular to the "surfaces." The

Schrödinger equation for the problem is

$$-\frac{1}{2} \nabla^2 \Psi_{\vec{k}}(\vec{x}) + V(x) \Psi_{\vec{k}}(\vec{x}) = \epsilon_{\vec{k}} \Psi_{\vec{k}}(\vec{x}), \quad (1)$$

with the potential

$$V(x) = \begin{cases} 0, & -L < x < L \\ V, & x < -L, \quad x > L. \end{cases}$$

The  $y$  and  $z$  coordinates are parallel to the surfaces, and periodic boundary conditions are applied to these coordinates. The wave functions for the problem have plane-wave form in the  $y$  and  $z$  coordinates with a period  $L$ :

$$\Psi_{\vec{k}}(\vec{x}) = (1/L) e^{i(k_y y + k_z z)} \psi_k(x).$$

The  $x$  component of the wave functions can be either even or odd:

$$\psi_{k_+}(x) = \begin{cases} (N_{k_+})^{1/2} \cos k_+ x, & -L < x < L \\ (N_{k_+})^{1/2} \cos k_+ L \exp[-(2V - k_+^2)^{1/2} |x - L|], & x < -L, \quad x > L \end{cases}$$

$$\psi_{k_-}(x) = \begin{cases} (N_{k_-})^{1/2} \sin k_- x, & -L < x < L \\ (N_{k_-})^{1/2} \sin k_- L \exp[-(2V - k_-^2)^{1/2} |x - L|], & x < -L, \quad x > L \end{cases}$$